


Multi-hazard risk to global port infrastructure and resulting trade and logistics losses

Jasper Verschuur ^{1✉}, Elco E. Koks^{1,2}, Sihan Li³ & Jim W. Hall¹

Despite their economic importance, the risk that ports face from multiple natural hazards has not yet been monetised on a global scale. Here, we perform an asset-level risk analysis of global port infrastructure from multiple hazards, quantifying the risk to physical asset damages and logistics services (i.e. port-specific risk) and maritime trade flows at-risk (i.e. trade risk). We find that 86% majority of ports are exposed to more than three hazards. Globally, port-specific risk totals 7.5 USD bn per year, with 32% of the risk attributed to tropical cyclone impacts. In addition, 63.1 USD bn of trade is at-risk every year, with trade risk as a fraction of total trade being particularly high in Small Island Developing States. Our result underline that port resilience is determined by various critical factors, such as engineering standards, operational thresholds, recovery duration, that vary widely across ports, requiring tailored solutions to improve port resilience.

¹Oxford Programme for Sustainable Infrastructure Systems (OPSIS), Environmental Change Institute, University of Oxford, Oxford, United Kingdom.

²Institute for Environmental Studies, Vrije Universiteit Amsterdam, Amsterdam, Netherlands. ³School of Geography and the Environment, University of Oxford, Oxford, United Kingdom. ✉email: jasper.verschuur@keble.ox.ac.uk

Ports are essential for the well-functioning of economies and global supply-chains^{1–3}. However, their strategic location along rivers and low-lying coastal areas makes them exposed to the impacts of climate extremes and natural disasters (e.g. extreme waves, cyclones, and earthquakes). For instance, Hurricane Ike (2008) caused an estimated 2.4 USD billion worth of damages to ports in Texas⁴, whereas the 2013–2014 floods in the United Kingdom damaged port infrastructure worth 1.8 GBP million⁵. The impacts of port disruptions are often felt beyond the port boundaries, as port closures can result in wider economic losses through maritime transport and global supply-chain networks that depend on ports' trade facilitation function^{2,6,7}. Given their economic importance and the large sums of money invested in port construction and operations from the private sector (around 92 USD billion since 1990 in low and middle-income countries alone⁸), combined with the predicted increase in natural hazard risk due to climate change^{9,10} and near tripling of maritime trade by 2050¹¹, detailed risk information at a global scale is essential to guide port infrastructure planning and investments and manage supply-chain risks.

Since ports form nodes in global networks of maritime supply chains, it is essential to take a global perspective to accurately estimate the risks from catastrophic port disruptions. However, the academic literature so far has inadequately addressed this. On the one hand, previous large-scale (continent or global) analyses have mainly looked at the exposure of ports to coastal flooding¹² or multiple operational thresholds from climate extremes⁹, with ports represented as single points. Although useful for analysing the frequency of occurrence of a single hazard or multiple hazards, these studies fail to quantify the economic damages to physical assets since asset locations (e.g. terminals, road, rail) are not included, nor the associated disruption pathways of port downtime and the losses associated with that (e.g. loss to trade, revenue, delays). On the other hand, a number of detailed (asset-level) port risk analyses, that include the different ways in which a port may be disrupted, have been performed, but only on a local scale covering one or a small subset of ports^{10,13,14}.

Despite the amount of work that has been done, we identified several remaining challenges to scaling up detailed risk analysis to a global scale. First, ports can be damaged or disrupted by several different hazards which impact the port's physical infrastructure and operations in different ways, making risk analysis complex. The risk profile of the port consists of both high-probability but low-impact events (e.g. operational disruptions due to weather extremes) and low-probability but high-impact events (e.g. a large-scale earthquake). Apart from impacts to the port assets themselves (e.g. cranes, terminals), ports are embedded in local critical infrastructure networks (e.g. rail, road and electricity), damages to which can halt port operations even if the port itself is not damaged. In fact, hazardous impacts to critical land-side infrastructure are identified as a key bottleneck for various ports, both in the developing and developed world^{10,13,15,16}. Incorporating this local complexity into a global analysis requires a large amount of local port-specific data, as well as incorporating a variety of port-specific hazards and failure mechanisms into a single risk framework. So far, this has been impossible given that (1) no global port asset database exists, (2) most studies ignore the link between port operations and the critical infrastructure networks they depend on and (3) global hazard datasets often have low resolution, making them incompatible with asset-level risk analysis, or requires additional local information (e.g. presence of a breakwater and depth of approach channel) to adequately capture the port's operational thresholds. On top of that, disruptions to trade flows going through ports can lead to additional logistics losses due to transportation delays, which can incur costs to those involved in facilitating logistics services (e.g.

port operators, carriers and shippers)^{17,18}. These losses could be substantial, as illustrated by the 2021 Suez blockage¹⁹, and could exceed physical asset damages. In order to quantify such additional trade and logistics losses, detailed information on port-level trade flows is needed, which is not yet readily available on a global scale. Hence, studies looking at logistics losses have only quantified the scale of these losses for the handful of ports for which such information is available¹⁷.

To bridge these gaps, this study presents the first asset-level risk analysis for 1340 ports globally, considering multiple hazards and failure mechanisms. We quantify both the physical damages to infrastructure assets as well as the associated logistics and trade at-risk due to port downtime (either due to asset reconstruction or operational thresholds). To do this, we create a new port infrastructure and land-use database that contains all the essential port infrastructure assets (terminals, breakwaters, cranes), critical infrastructure assets (road, rail, electricity transmission, power generation), and industrial facilities within the immediate port area (defined as the 1 km buffer around the port terminals). Our risk framework includes both operational disruptions to ports (that do not cause damages), which typically occur due to extreme wind, temperature, wave heights and overtopping, as well as the physical damages to port infrastructure as a result of natural hazards from tropical cyclones (TCs), earthquakes, river flooding, pluvial flooding and coastal flooding. Using a fault tree methodology, we capture how multiple failure pathways can result in impacts on the port's operational status. Moreover, by combining our risk estimates with a recently developed port-level trade network, which was constructed from a big dataset of vessel Automatic Identification System (AIS) observations¹, we estimate the amount of trade disrupted and the additional logistics losses to port operators (revenue losses), carriers (losses of late delivery) and shippers (inventory costs and value of time) (Methods).

To investigate the factors that drive the calculated risk estimates, and to account for the many uncertainties associated with such a global analysis, we perform a large-scale sensitivity analysis that covers, among others, the uncertainties associated with the resilience of ports. Port resilience, which reflects the ability to prevent, cope and recover from external disturbances²⁰, is incorporated in our framework by varying the engineering design standards (e.g. susceptibility of port infrastructure to damage during extreme conditions), reconstruction costs of port and critical infrastructure assets (which can vary significantly across ports), and the measures in place to improve operability during extreme conditions (e.g. pilot vessels and tug boats that can cope with larger wave heights) or shorten the recovery time after disruptions (e.g. business continuity plans). As well as providing an uncertainty range associated with our risk estimates, the sensitivity analysis thus provides insights into how various ports can benefit from further investments or operational adaptations to improve resilience, or, on the other hand, how the decline of resilience in the future will worsen the risk of port failures.

Altogether, the analysis presented in this work is the first comprehensive overview of natural hazard risk to ports on a global scale, providing essential insights for policymakers, private-sector investors, insurance companies and other maritime stakeholders. It further sets the scene for analysing changes in risk due to climate change and the need for port expansions, as well as performing adaptation analysis.

Results

Overview. The multi-hazard risk framework includes both the extremes that most disrupt port operations (extreme wind, temperature, waves and overtopping), hereafter referred to as maritime extremes and the natural hazards that can cause the

physical failure of the port infrastructure (cyclone wind, earthquakes, river flooding, pluvial flooding and coastal flooding). We adopt two risk metrics throughout the port-specific risk and the trade risk, both measured in monetary value.

Port-specific risk is the sum of three types of impacts incurred by the actors who own, operate and use ports: (1) the physical damages to port infrastructure (e.g. terminals, cranes and industrial facilities), (2) the physical damages to critical infrastructure in the port vicinity (electricity, road, rail and power plants) upon which the port depends and (3) the additional logistics losses to port operators, carriers and shippers as a result of downtime due to the exceedance of operational thresholds or asset reconstruction (see Methods). Although port infrastructure is considered a critical infrastructure itself, in this study, we refer to critical infrastructure as the dependent critical infrastructure to support the efficient functioning of the port, including road, rail and electricity generation and transmission infrastructure.

Disruptions to trade flows can have wide-scale economic impacts, by impacting supply chains, within or across borders, that are essential for the production and consumption of goods^{2,21,22}. The likelihood of such trade bottlenecks is related to the frequency and duration of port downtime and the flow of goods through ports that are potentially disrupted. Therefore, we define trade risk in this paper as the amount of trade (measured in monetary value) that is expected to be disrupted (or at risk) by natural hazards and maritime extremes on an annual basis (see Methods).

Throughout this paper, for both port-specific risk and trade risk, we report the median risk estimates and the confidence interval (CI: 5–95th percentile) as found by performing the sensitivity analysis (see Methods).

Multi-hazard exposure. Most ports are exposed to damages and disruptions from a multitude of extremes and natural hazards. 40.1% (22.1–63.1%) of 1340 ports are exposed to extreme maritime conditions that surpass the operational thresholds. The vast majority of ports (94.8%) are exposed to more than one natural hazard, with 50% of ports being exposed to 4 or 5 natural hazards. Fluvial and pluvial flood hazards are most prevalent, with 80.4% (70.9–81.4%) and 84.3% (57.8–88.2%), of ports, respectively, being exposed to these natural hazards. Some of the hotspots of multi-hazard exposure are in Japan, the West Coast of the United States and Middle America, New Zealand, Taiwan and parts of mainland China (Supplementary Fig. 1a). Ports in South America, parts of Northern, Western and Eastern Africa, and Northern and Eastern Europe are only exposed to two or fewer hazards (Supplementary Fig. 1b). Hence, the vast majority of ports need to consider multiple hazards in the design and operations of infrastructure. For instance, the foundations of quay walls need careful consideration when exposed to earthquakes, the orientation and design of breakwaters when exposed to extreme waves and surges, and the drainage system when exposed to fluvial and pluvial flooding.

The spatial footprint of port-specific risk. Figure 1a shows the expected port-specific risk and the dominant hazard (colour of the dot), while Supplementary Fig. 2a–f shows the port-specific risk estimates per hazard. On a global scale, the median port-specific risk is found to be 7.6 (4.0–17.4) USD bn per year (histogram Fig. 1A). The largest port-specific risk is attributed to TCs with a median risk of 2.4 (0.7–12.2) USD bn per year, followed by fluvial flooding 1.9 (0.7–12.2) USD bn per year, coastal flooding 0.8 (0.5–1.23) USD bn per year, pluvial flooding 0.7 (0.2–1.6) USD bn per year, operational exceedances 0.5 (0.06–2.4) USD bn per year, and earthquakes 0.2 (0.1–1.3) USD bn per year. The

relative importance of the different hazards on a port level, however, varies geographically (colour dots in Fig. 1a). TC is the leading hazard globally (for 25.2% of ports), in particular for the Caribbean, Eastern Asia and Northern Australia, whereas fluvial (22.6%) and coastal flood (23.7%) are the leading hazards for Western and Northern Europe. The spatial footprints of port-specific risk contributed by flooding are driven by the location of rivers and occurrence of extreme coastal water levels on the one hand, and the local presence of flood protection standards, or lack thereof, and the freeboard of the terminals on the other hand. Although the earthquake-induced risk is small overall, earthquakes are still the leading hazard for 10.8% of the ports, with hotspots found in Chile, parts of the Mediterranean and Northern Japan. In some countries, such as India, the United States and Australia, different dominant hazards are identified across the country, emphasising that port-specific risk is determined by the local conditions and. As such, it is essential to perform a local risk analysis that take the multiple hazards into consideration in a unified risk framework.

Figure 1b shows the top 50 most at-risk ports globally in terms of expected port-specific risk. The largest port-specific risk is found for ports in Asia, in particular located in mainland China and Taiwan (China), ports in the Gulf of Mexico, and ports in Western Europe. The ports of Houston (United States, 169.0 USD m per year), Shanghai (mainland China, 133.2 USD m per year), Port Elizabeth (South Africa, 123.4 USD m per year), Lazaro Cardenas (Mexico, 110.9 USD m per year) and Rouen (France, 98.7 USD m per year) are found to be the top 5 at-risk ports. The port of Houston faces the largest risk from a combination of cyclone wind, pluvial flooding and fluvial flooding, whereas, for the port of Shanghai, cyclone wind is by far the most important hazard. Fluvial flooding is the dominant hazard for the ports of Rouen and Lazaro Cardenas, while the exceedance of operational thresholds, in particular from extreme wave heights, contributes most to the port-specific risk for Port Elizabeth. Around half the ports globally face risk larger than 1 USD m per year, with 160 ports facing moderately high risk (10 USD m per year) and 21 ports facing very high risk (>50 USD m per year). Most of the top 50 ports are very large ports in terms of estimated freight flows (>10 USD bn annually), therefore having large port areas exposed.

To put this number into perspective, the port-specific risk is expressed in terms of the risk per square metre of port area (referred to as relative risk hereafter), and grouped according to the income level of the country (following the World Bank Income Classification). Ports in high-income countries face a relative risk of 123.4 (55.7–379.5) USD per year, which is slightly higher than ports in low-income countries (117.7, 45.7–312.1 USD per year) and upper-middle-income countries (118.4, 53.3–404.7 USD per year), but lower than ports in lower-middle-income countries (155.5, 87.4–377.6 USD per year). Therefore, despite the absolute risk being particularly large in high-income countries, ports in high-income countries have the financial resources to take protective measures (e.g. higher flood protection standards, elevated terminals) to reduce risk in relative terms, compared to lower (and) middle-income countries. A similar observation can be made for the port-specific risk to global road and rail infrastructures²³.

Contribution risk factors to port-specific risk. The three different risk factors (port infrastructure damages, critical infrastructure damages, and logistics losses) contribute to the port-specific risk to various extents. Physical damages to port infrastructure are responsible for 58.6% of the port-specific risk to ports globally, followed by logistics losses (22.2%) and critical infrastructure damages (19.2%) (Supplementary Fig. 3).

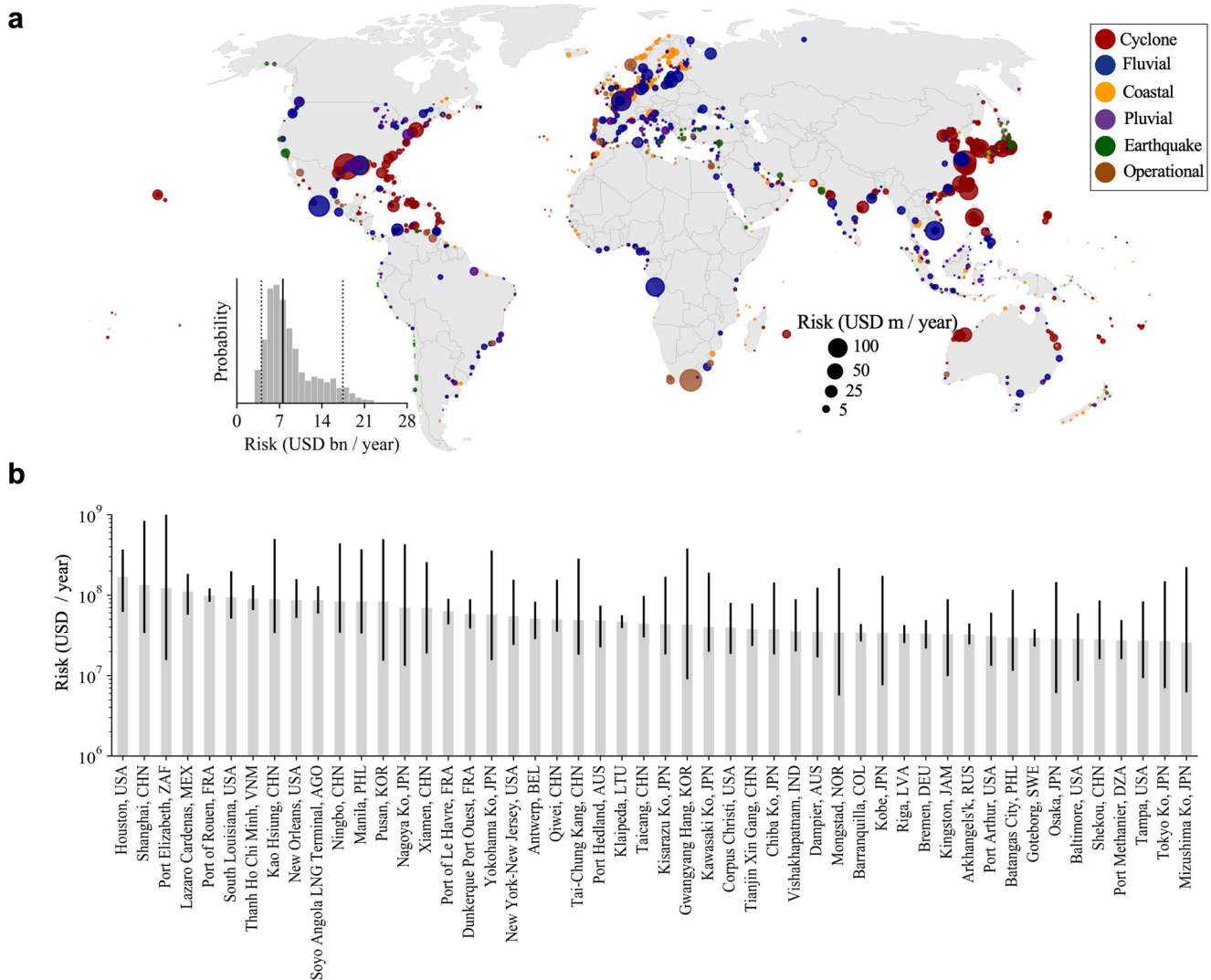


Fig. 1 Global footprint of port-specific risk. a The median risk per port is expressed in USD m per year, with the colour indicating the dominant hazard. The histogram illustrates the globally aggregated risk across the 10,000 samples, with the black line indicating the median and the dashed lines indicating the 5th and 95th percentiles. **b** The top 50 ports in terms of median expected risk (bars). The error bars reflect the 5–95th percentile of the risk estimates based on the 10,000 samples. Note the logarithmic y-scale.

TCs wind, causing frequent downtime to ports²⁴, is the hazard that causes most logistics losses. Of the cyclone-induced risk, 30% are logistics losses, while for the other natural hazards, logistics losses are small relative to port infrastructure and critical infrastructure damages (ranging from 1.2% for earthquakes to 8% for fluvial flooding). In contrast, for coastal, pluvial and fluvial flooding, critical infrastructure asset damages contribute 28.2%, 24.5% and 22.8%, respectively, to the port-specific risk of these hazards on a global scale (Supplementary Fig. 3).

Figure 2a–c illustrates the relative importance of the three risk contributors per port, showing how the damages to port infrastructure dominate the port-specific risk. Still, the risk to critical infrastructure assets is the largest contributor to port-specific risk for ~12% of the ports globally, particularly centred in Europe and the United States. This result resonates with the previous work^{10,13,15}, illustrating that critical infrastructures in the vicinity of ports are essential to consider in risk analysis and adaptation strategies, as they are often more exposed to fluvial and coastal flooding (given that port terminals are often built to higher elevations hence less vulnerable in comparison). Logistics losses are large for ports with large throughput quantities that are

exposed to maritime extremes and TCs, both resulting in large disruptions if ports have to shut down without major damages to infrastructure assets. Examples are Port Hedland and Port Walcott in Australia, Saldanha Bay and Port Elizabeth in South Africa, and Ulsan and Incheon in South Korea (all >70% of port-specific risk).

Figure 2d–f shows the absolute and relative port-specific risk (risk per unit port area) broken down by the size of ports (four quantiles based on the port area—small/medium/large/very large as shown in Fig. 2d–f) and income groups. For the port infrastructure, although the absolute risk is largest for the very large ports in high-income countries, the relative risk is highest for small ports in low-income countries. The high absolute port infrastructure risk in high-income countries is in line with the expectation that more developed countries trade more and need larger port areas to facilitate the trade flow, leading to a larger number of assets at risk. In general, however, larger ports face a lower relative risk, although the differences are small across income groups and port sizes. The decrease in relative risk with income groups can be explained by the difference in exposure but is more likely due to the fact that higher-income countries

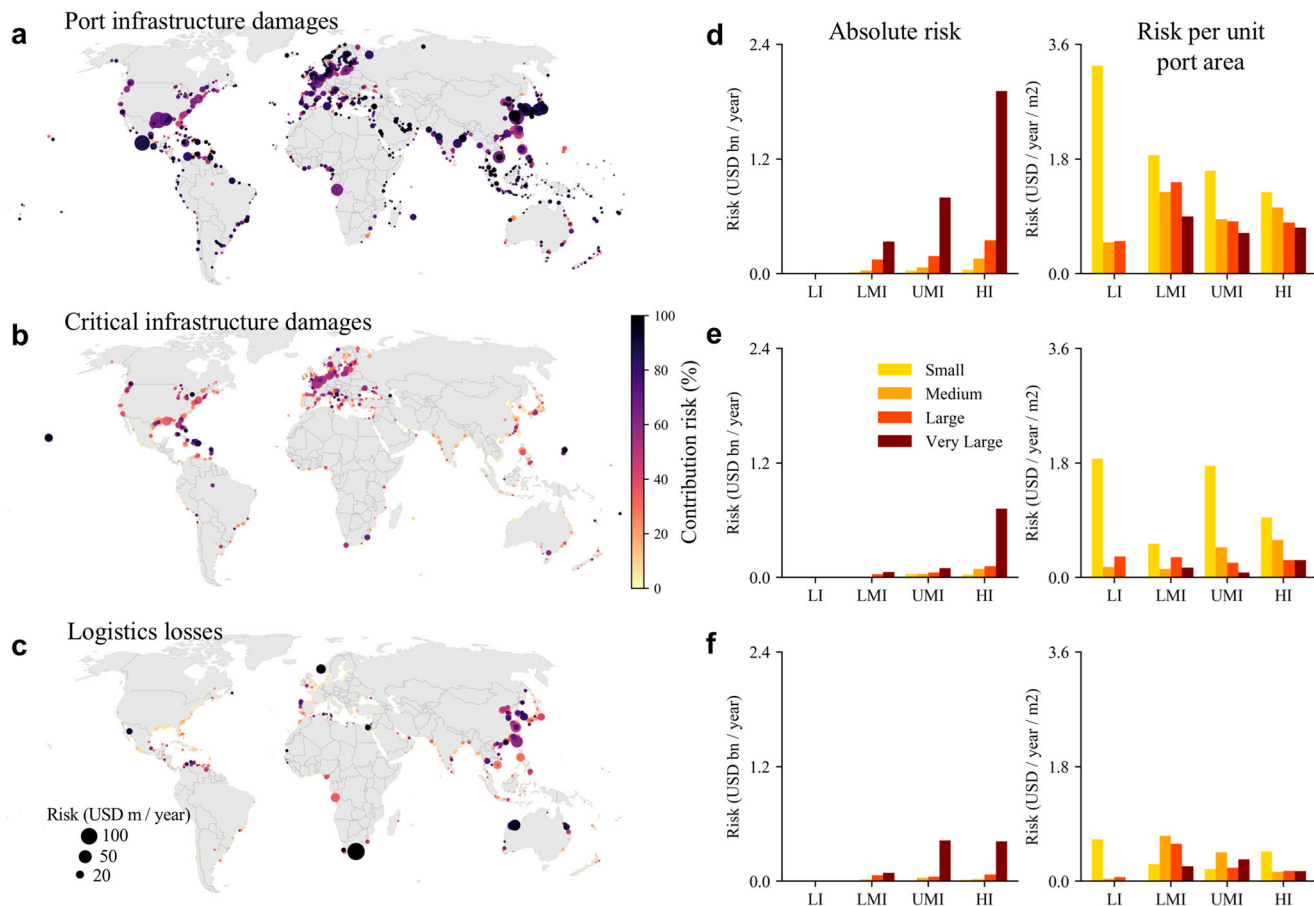


Fig. 2 Contribution of different hazards to expected port-specific risk. **a** The contribution to the risk is due to physical damages to port infrastructure. The colour indicates the fraction of contribution, whereas the size of the marker denotes the risk. **b** Same as **(a)** but for physical damages to critical infrastructure. **c** Same as **(a)** but for the logistics losses. **d** On the left, the absolute risk due to the physical damages to port infrastructure, grouped by the size of the port (based on four quantiles of the total port area mapped) and the level of income of the country (based on the World Bank Income Classification), is shown. On the right, the relative risk (per square metre of port area) is shown. **e** Same as **(d)** but for physical damages to critical infrastructure. **f** Same as **(d)** but for the logistics losses. All values reflect the median estimate across the 10,000 samples.

have the financial resources to invest more in flood protection (both river and coastal) or elevate their port terminals. For critical infrastructure, the larger ports in high-income countries face the largest absolute risk, whereas, the small ports in both low-income and upper-middle-income countries face a high relative risk (Fig. 2e). The absolute critical infrastructure risk is almost negligible for small ports, especially in low-income countries, with tertiary or secondary roads providing transport connectivity, which has lower replacement costs. However, small ports have higher relative critical infrastructure risk as they often only have one or two main transport or electricity infrastructure networks connecting to the port, making them more vulnerable if these assets are hazard-prone. Contrary to the above, the absolute risk as a result of logistic losses (Fig. 2f) is largest in very large ports in upper-middle-income countries. The relative risk is less related to the size of the port, with both large and small ports across the income groups facing almost equally large relative risk.

Spatial distribution of trade risk. Figure 3a shows the global distribution of trade risk (measured in monetary value) for all the ports. On a global scale, the trade risk is estimated to be 66.9 (47.1–109.7) USD bn per year (histogram Fig. 3a). In other words, around 0.80% (0.53–1.76%) of the total maritime trade value is at-risk every year of being disrupted due to natural

hazards and maritime extremes. Locations of high trade risk are concentrated in the cyclone-prone areas of East Asia, where hazard-induced port downtime disrupts large trade flows. A total of 27 ports are associated with a trade risk of >0.5 USD bn per year with the ports of Shanghai (mainland China), Ningbo (mainland China), Kaohsiung (Taiwan, China), Xiamen (mainland China), and Busan (South-Korea) having the highest trade risk globally.

On an aggregated level (e.g. country and economic entity), the trade risk denotes the total amount of trade measured in monetary value that could be disrupted on an annual basis. Small Island Developing States (SIDS), whose economies are critically dependent on maritime transport¹, face disproportionately high trade risk, which is 3.7 times higher than non-SIDS economies (Rest of World, in Fig. 3b) on average (averaged across economic entities). In line with the port-specific risk estimates, lower-middle-income countries are found to be faced with the largest trade risk on average, while trade risk is small for low-income counties (Fig. 3c). The Northern Mariana Islands (1.8%, 1.1–4.0%), Guinea-Bissau (1.7%, 0.1–6.9%), Guam (median 1.5%, 5–95th CI: 0.9–3.5%), Philippines (1.3%, 0.9–2.9%), Saint Vincent and the Grenadines (1.2%, 0.8–2.0%), and Dominica (1.2%, 0.9–2.2%) face the largest risk of trade bottlenecks, due to the large concentration of trade through at-risk ports (top 30 economies shown in Fig. 3d).

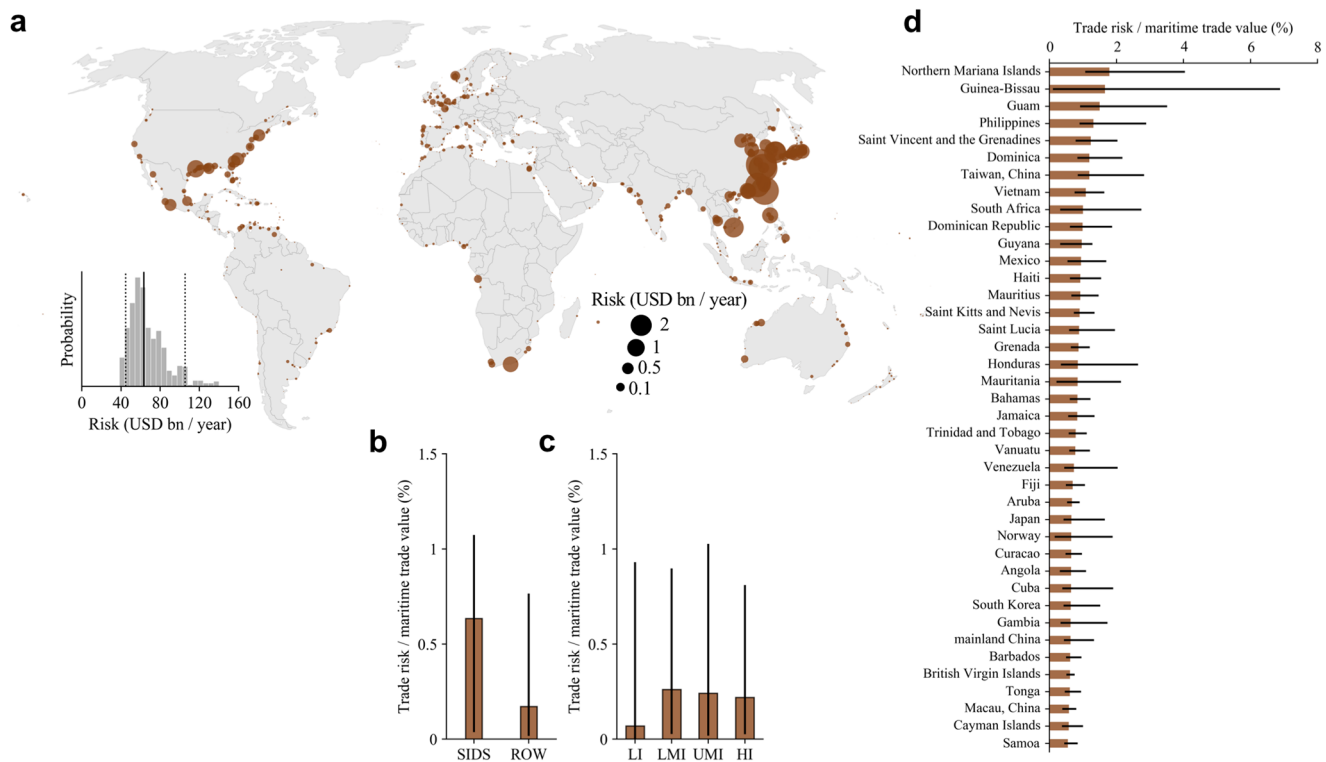


Fig. 3 Global footprint of trade risk. **a** The median trade risk is USD bn per year, reflecting the risk of trade disruptions as a result of downtime per port. The histogram illustrates the global aggregated trade risk across the 10,000 samples, with the black line indicating the median and the dashed lines indicating the 5th and 95th percentiles. **b** The distribution of the trade risk over Small Island Developing States (SIDS) and Rest of World (ROW) countries, with the bar showing the median across countries and the error bar at the 5 to 95th percentiles. **c** Same as (**b**) but for countries grouped by the different income groups. **d** The trade risk is expressed as a percentage of the annual maritime trade value. The top 40 economies are depicted with the error bar indicating the 5-95th uncertainty range across the 10,000 samples.

Sensitivity analysis. Uncertainties are prevalent throughout the analysis and are investigated through variance-based sensitivity analysis (see Methods). This allows us to explore the main parameters driving the variance in both port-specific risk and trade risk estimates (see SI Appendix for a discussion). Moreover, it elucidates the uncertainty in the risk estimates on a port level, as these sensitivities are not uniform across the ports. Figure 4a illustrates the relative uncertainty estimates of the port-specific risk (expressed as the 5–95th uncertainty range over the mean value), showing that large relative uncertainties are prevalent in Africa, the Middle East and East Asia. These differences in the uncertainties illustrate that part of the port-specific risk is unavoidable, or insensitive to parameter input, whereas part of the port-specific risk is associated with the sensitivity of some key parameters, especially those reflecting the current level of resilience of the ports. Figure 4b also shows the relative uncertainty estimates for the trade risk estimates, which are overall higher than the port-specific risk and have a different spatial pattern. For trade risk, large relative uncertainties are identified in Northern Europe, Africa, South America and the Mediterranean, whereas the tropics present relatively low uncertainties. This is mainly associated with the uncertainties in downtime as a result of TCs, which are relatively small in our empirically based modelling framework as they are often unavoidable (see Methods).

The resilience level of a port determines its risk profile. Resilience, in our analysis, includes the capacity of ports to operate under more extreme maritime conditions, the ability of ports to cope with hazard impacts (e.g. through improved engineering standards of infrastructure), and the measures in place to quickly recover after a hazard, thereby shortening the

recovery duration (e.g. lead times of asset replacement, emergency preparedness). Given that the level of resilience is impossible to measure in a generalised way on a global scale, the sensitivity analysis helps to provide insights into how slight improvements or the deterioration of, port resilience can influence port-specific and trade risk. Figure 4c–h illustrates the contribution of the engineering standards, recovery ability and operational resilience to the overall variance in the risk results. For the vast majority of ports, the port-specific risk estimates are mainly influenced by the engineering standards of the port and critical infrastructures (Fig. 4c), and only a small number of ports are influenced by the recovery ability (Fig. 4e). The importance of engineering designs was also identified as a major uncertainty in previous large-scale infrastructure risk analysis^{23,25}. Operational resilience, however, is very important for a number of ports, in particular those showing large relative uncertainties (Fig. 4g). This illustrates that for these ports, being resilient against maritime extremes, e.g. improved operability under extreme winds and waves, is a key factor in the overall risk these ports face. For instance, for Port Elizabeth, which faces potentially frequent operational disruptions due to its high exposure to extreme waves, being able to operate under higher waves heights (e.g. tugs and pilot vessels that can cope with this) will diminish the frequency of disruptions as a result of exceedance of operational thresholds. This also underlines that these ports are sensitive to changes in these extreme conditions as a result of climate change.

Trade risk is sensitive to a more complex combination of contributors to resilience. In particular, the engineering standards are still important for cyclone-prone areas (Fig. 4d),

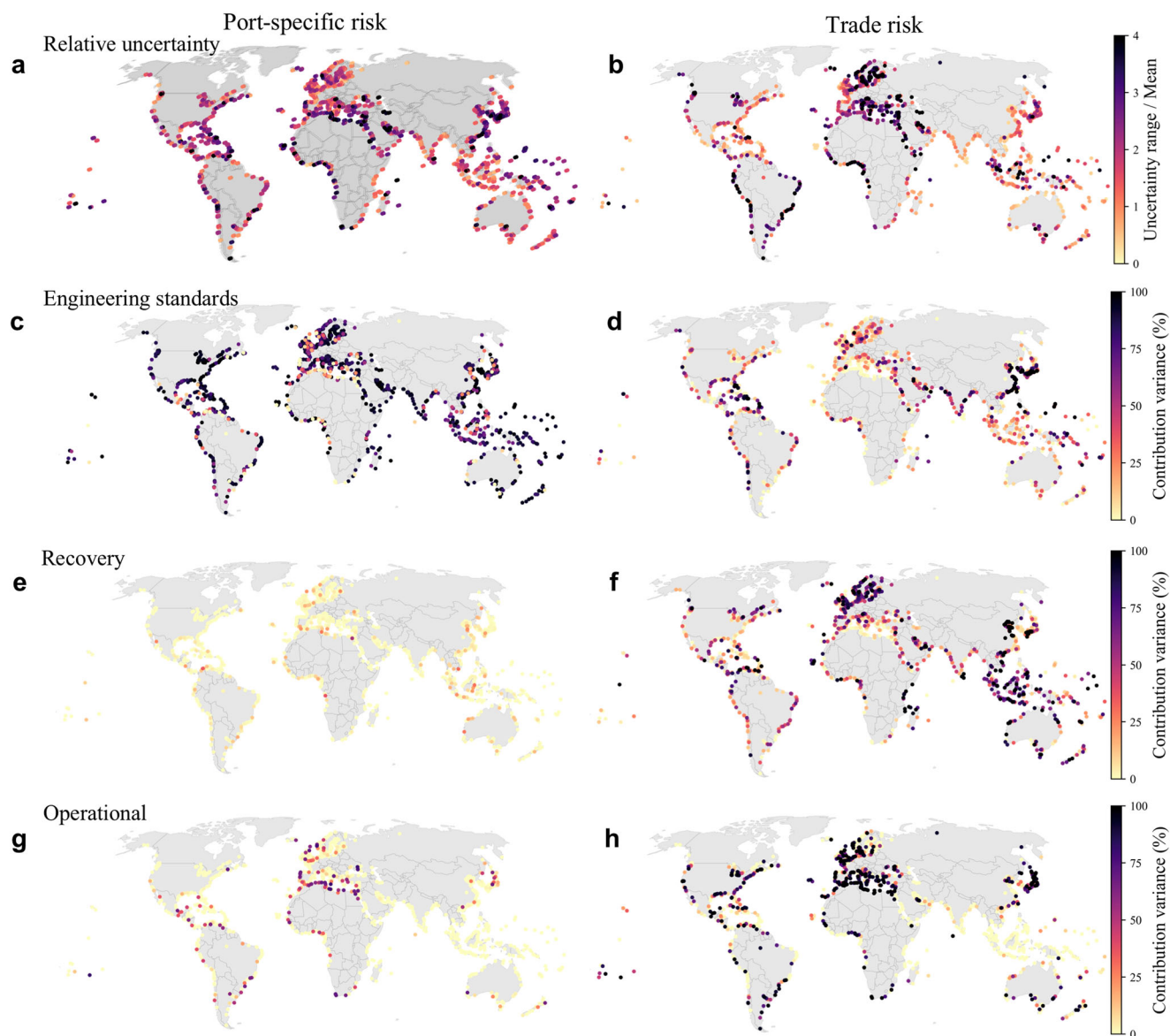


Fig. 4 Uncertainty range and sensitivity analysis of resilience parameters. **a** The relative uncertainty, expressed as the 5–95th uncertainty range over the mean, over the 10,000 model realisation for the port-specific risk. **b** Same as **(a)** but for trade risk. **c** The contribution of the input parameters reflects the uncertainty in the engineering standards of ports with respect to hazard impacts (depth-damage curves) to the port-specific risk model variance. **d** Same as **(c)** but for trade risk. **e** The contribution of the input parameters reflects the uncertainty in the recovery ability of ports with respect to hazard impacts (recovery curve, maximum recovery duration) to the port-specific risk model variance. **f** Same as **(e)** but for trade risk. **g** The contribution of the input parameters reflecting the uncertainty in the operability of ports with respect to climate extremes (wave height, wind, temperature and overtopping) to the port-specific risk model variance. **h** Same as **(g)** but for trade risk.

while recovery ability and operational resilience are dominant drivers of uncertainty in other parts of the world (Fig. 4f, h). Hence, whereas reducing the recovery duration and improving operability against climate extremes have limited effect on the port-specific risk (as logistics losses are relatively small), they are essential for the trade risk as they directly influence downtime. In light of these results, collecting local information on operational thresholds, recovery ability, and engineering standards is extremely important to refine the risk estimates. For instance, a port survey by UNCTAD²⁶ illustrated that operational thresholds can vary considerably across ports, with critical wind thresholds varying by a factor of two to three between ports and critical coastal flood thresholds for the continued integrity of the ports ranging from zero to five metres.

Discussion

This paper presents the first comprehensive and systematic multi-hazard risk analysis of ports on a global scale, quantifying the physical damages to port and critical infrastructure assets, and logistics and trade losses due to natural hazard-induced port downtime. We find that most ports are exposed to several hazards that can cause large damages and disruptions. Globally, 86.2% of ports are exposed to more than three hazards, while around a fifth of the ports is prone to the impacts of five or six hazards (out of the six hazards considered). The large exposure of ports in north-western Europe to coastal flooding is in line with the work of Christodoulou et al.¹², who also identified this region as highly exposed to present-day extreme water levels (EWL). The results presented by Izaguirre et al.⁹, although mainly looking at operational thresholds of ports and not natural hazard impacts,

show a similar pattern of high multi-hazard exposure in Japan, South-East Asia, the Caribbean, and parts of Mexico. However, the inclusion of fluvial flooding, pluvial flooding and earthquakes in our study brings additional nuances to the spatial distribution of natural hazard exposure.

Our results underline that port risk analysis should not just focus on a single hazard, but should take a multi-hazard perspective. However, in the current analysis, while considering multiple hazard types, we do treat hazard occurrence as independent, as non-linear hazard interactions are ignored. Therefore future analysis should consider how these hazards may combine into compound²⁷ and/or consecutive disasters²⁸, or how multiple ports can be disrupted simultaneously²⁴, in particular when multiple hazards are driven by the same large-scale synoptic weather systems (e.g. winter storms in Europe). Moreover, hazard risk associated with tsunamis is not included in the present methodology. Despite promising developments in providing global tsunami hazard data^{29,30}, global tsunami risk modelling is still at its infancy. However, while considered low-probability events, the impacts of tsunamis on port facilities can be considerable, as exemplified by the 2011 Tohoku earthquake and subsequent tsunami in Japan, with total tsunami-induced physical damages to the Japanese maritime sector (vessels, ports and maritime facilities) approximated to be 12 USD billion³¹.

The port-specific risk from damage and disruption at ports is found to be 7.6 (5–95th CI: 4.0–17.4) USD bn per year, mainly driven by cyclone wind and flooding (fluvial, coastal and pluvial). This global number is over half as large as a previous estimate of the physical asset risk of road and rail infrastructure on a global scale²³, illustrating that although ports only encompass relatively small areas, the high value and density of assets can contribute to the natural hazard risk to critical infrastructure on a national and global scale.

Out of the 1340 ports studied, 160 ports face a risk of more than 10 USD m per year, while 21 ports face a risk of more than 50 USD m per year. In absolute terms, the port-specific risk is concentrated in the large ports in high-income countries, given their extensive port areas and high infrastructure density, whereas the risk relative to port area is higher in small ports in low-income countries. This poses a twin problem. On the one hand, large ports need to make sizeable investments to manage their risk in light of increasing climate change. For instance, by 2100, 12–63 USD bn is needed to elevate port terminals to accommodate rising sea levels³², which is already several times higher than the port-specific risks estimated in this study. On the other hand, infrastructure upgrades are needed to protect small ports in low-income countries from hazard impacts and frequent disruptions, which can have systemic impacts on economic growth in these countries³³. At small ports, the impacts of climate change on economic activity can be reduced by improvements to infrastructure to make them more disaster-resilient and ensure year-round operations. For instance, the Asian Development Bank-financed several investment proposals to upgrade some of the outdated port infrastructures in Papua New Guinea (replacing and raising the deck in Alotau port), Samoa (rehabilitating the breakwater, upgrading terminal infrastructure and upgrade of tug boat of Apia port) and Niue (redesigning the wharf of Alofi port)³⁴.

Although damage to port infrastructure is the main contributor to port-specific risk across ports, logistics losses and critical infrastructure damages cannot be ignored. For instance, risk due to critical infrastructure is large in Europe and North America, mainly as a result of flood impacts that can cause bottlenecks to port functionality if critical infrastructure networks are disrupted. Flood risk management of critical infrastructure assets in the port's vicinity should therefore be an integral part of risk

management. However, given that the ownership of port terminals (e.g. often owned by a terminal operator) and critical infrastructure (e.g. often owned by national or city governments) differ, and hence responsibilities for risk management, creating a port-wide risk strategy is essential to avoid misalignment between risk standards.

In addition to the potential for damage and losses at and around ports, we find that 0.8%, but up to 1.8%, of global maritime trade, is at-risk from disruptions every year. In particular, SIDS are prone to trade risk, but also larger economies such as Taiwan, the Philippines and Vietnam. Cyclones are the main contributor to trade risk, as they can cause frequent downtime to ports, in line with the previous literature^{9,17,24}. Such maritime trade disruptions can further cause supply-chain losses on a global scale, which are not quantified in this study but can be equally large or even larger than the asset damages²². For instance, a previous study has estimated that every dollar of maritime trade is associated with 4 dollars of global economic activity¹, emphasising that supply-chain losses can be substantial, but are highly dependent on the resilience embedded in both the maritime network and economic system^{2,6}.

Finally, the sensitivity analysis not only highlights that the risk estimates are sensitive to the input parameters, but that the importance of certain parameters, especially the parameters reflecting the ports' resilience to hazard impacts, differs per port and risk metric. Efforts to assemble and share such resilience information, as already done by organisations such as PIANC (for instance, the 'Navigating a Changing Climate' initiative) and UNCTAD (such as 'Port Industry Survey on Climate Change Impacts and Adaptation'²⁶), should be enhanced in order to improve risk estimates and learn from best practices.

This study has demonstrated that it is now feasible to perform an asset-level risk analysis on ports on a global scale as a result of newly developed global datasets of port assets, hazard information at a port level, and a new port trade database. This can help understand the scale and spatial footprint of risk, and facilitate the prioritisation of investment needs. Such information is highly relevant for a variety of stakeholders involved in the maritime supply chain, including policy-makers, private-sector investors, insurance companies, and maritime operators. Moreover, this research paves the way for a complete assessment of the natural hazard risks to global maritime trade and supply chains as a result of climate change. Further incorporating climate change into our unified analysis framework will enable quantification of the scale of global investment that will be required in adaptation measures, such as elevating port terminals, improving flood protection standards, or enhancing port-level resilience (e.g. retrofitting port infrastructure).

Methods

Overview. The methodology includes the following components: (1) the creation of a database of port and critical infrastructure, (2) the assumptions and approach for deriving the operational thresholds, (3) the assumptions and approach for performing the physical asset damage analysis and recovery duration for the five natural hazards (coastal flooding, river flooding, pluvial flooding, cyclone wind and earthquakes), (4) the assumptions and approach for performing the fault tree analysis (FTA) to estimate the port downtime, (5) the assumptions and approach for estimating the logistic losses, (6) port-specific risk and trade risk estimation and (7) the methodological approach for incorporating the variance-based sensitivity analysis in the risk framework. An overview of all the input parameters and model assumptions is included in Supplementary Table 1.

Port and critical infrastructure database. The port and critical infrastructure database consist of the following assets: (1) port terminals and associated land-use, (2) critical infrastructure including road, rail, electricity transmission lines and power plants, and (3) an estimated number of ship-to-shore cranes for container terminals. First, we manually mapped and classified more than 13,000 land-use areas across all ports considered using satellite imagery available in QGIS software (Google Satellite). We classified port land-use areas into 15 port land-use types,

which we further aggregated into seven main types (Container, Dry Bulk, General Cargo, Liquid, RoRo, Storage, and Other). These land-use types are chosen as they can be easily distinguished from imagery, require specific handling equipment and have different reconstruction costs. Supplementary Table 2 provides an overview of the port land-use types, and Supplementary Fig. 4 gives examples for each port land-use type. The industry is often clustered around port areas or integrated within the port boundaries. We extracted the industrial land-use layer (polygons) included in OpenStreetMap (OSM) and manually checked if all industry were included. If the industry is missing, we supplemented the OSM data with manually mapped industry polygons. In total, over 2000 industrial facilities are located in the vicinity of ports in our database. The land-use types Container, Dry Bulk, General Cargo, Liquid and RoRo are considered the essential port land-use types for operational purposes. Only in case, ports have one industry land-use (and no port land-use), the ‘industry ports’, we considered this industry as the essential land-use for port operations. A breakdown of port areas per continent and a comparison with previous work are included in the Supplementary Methods.

Second, we included critical infrastructure assets within the port vicinity in the risk analysis. For every port, we added a buffer with a 1-km radius to the port and industrial land-use areas, which we define as the vicinity of a port. We also tested other buffer areas (0.5–5 km), with 1 km being a compromise between including too many infrastructure assets (especially for ports close to city centres) or including too little (for ports in more remote areas). We hereby assume that these assets are critically important for the well-functioning of the port. Within this buffer, we extracted the asset locations of roads from the GRIB database³⁵, rail networks from OSM data, electricity transmission lines from Gridfinder³⁶ and power plants from multiple external databases, including the WRI global power plant database³⁷ and a global coal power plant database³⁸.

Third, we estimated the number of ship-to-shore cranes needed for container (off)loading, as they are susceptible to cyclone wind damage. The number of cranes is derived by first capturing the maximum daily number of container vessels per port (based on data reported in³⁹) and multiplying this with the average number of cranes needed per vessel (see Supplementary Table 1).

In Supplementary Fig. 5, examples of geo-located ports and critical infrastructure assets for six ports are shown.

Operational risk analysis. For the operational risk analysis of ports, we include wind speed, temperature, wave height and wave overtopping (referred to as maritime extremes), similar to Izaguirre et al.⁹. We evaluated the average number of days per year, a critical operational threshold is exceeded, which is the operational risk of downtime, and added the four downtime measures up to come up with the total operational downtime. We hereby assume that the exceedance of an operational threshold leads to the closure of a port without any physical damage to the port or critical infrastructure.

The operational thresholds for temperature and wind have been derived in the previous work⁹ and confirmed by port experts and other research^{24,40}, with the threshold for wind speed set at 17 m/s and for temperature set at 35 °C. However, for temperature, we add a threshold of 45 °C for countries in the Middle East to reflect the local operational conditions. The wind threshold reflects the operational threshold of cranes in ports. The threshold for temperature reflects that at this temperature, ports face a daily productivity loss as outside workers have to take mandatory breaks or suspend operations, alongside potential melt of tarmac surfaces at the wharves. In contrast to the other threshold in the analysis, where we assume a full day of operational downtime for the temperature threshold, we assume that exceeding this threshold results in a three-hour loss in daily productivity. To get the exceedances of wind and temperature, historical time series (1979–2018) at every port centroid are extracted from ERA5 global reanalysis data⁴¹.

For waves and overtopping, we adopt two thresholds (normal exposure (NE) and high exposure (HE)) based on the exposure level of the port, the distance to the coast, and the type of coastal protection in place (e.g. natural protection, breakwater, seawall). To get information on the breakwaters, we manually mapped and classified breakwaters from satellite imagery (classified as either coastal breakwater, seawall or inlet) for all ports in our sample (see Supplementary Methods for a description). First of all, ports that are located inland (defined as being at least 20 km from the coastline) are not exposed to the impacts of sea waves and overtopping (some may be exposed to locally generated waves, but these are not included in the wave data). Second, ports that have an inlet breakwater are exposed to wave heights, but not to overtopping (since the port infrastructure is located inland). Third, ports that have a shelter characterised as ‘Excellent’ or a port type characterised as ‘River Tide Gates’, ‘Coastal Tide Gates’ or ‘Coastal Natural’ in the World Port Index (WPI), without an engineered breakwater, are assumed to be well sheltered and not exposed to waves and overtopping. All remaining ports are assumed to be exposed to waves and are assigned the NE threshold, except ports that are considered an ‘Open Roadstead’ type in the WPI, which are assigned the HE threshold, since they have no natural or engineered protection. For overtopping, all coastal breakwaters are assigned the NE threshold, while ‘Open Roadstead’ ports and seawalls are assigned the HE threshold.

For waves, the NE threshold is set to five metre and reflects the operational thresholds of pilot boats and safe manoeuvring of vessels when entering harbours, with coastal protection preventing wave penetration inside the sheltered area. The HE threshold is set for ports where port operations and cargo handling is directly

exposed to wave impact (e.g. some oil terminals). Here, we adopt a threshold of four metre, above which vessel (un)loading is limited. For wave overtopping, we set the wave overtopping threshold based on the type of coastal protection. A tolerable overtopping criterion of 0.4 l/s/m is adopted for seawalls⁴² and 1 l/s/m for breakwaters⁴³. Seawalls often have port equipment or other critical port assets located directly behind the seawall and are therefore engineered with lower overtopping limits⁴³.

To derive the annual exceedances of wave and overtopping thresholds, additional processing steps are needed. We extracted wave parameters (significant wave height, wave period and wave direction) from ERA5 global reanalysis wave data at 6-h intervals from 1979 to 2018⁴¹. For every port, we extracted data at the closest grid cell and created a daily time series by selecting the wave parameters concurrent with the daily maximum wave height. This wave height is then propagated to the entrance of the port based on a simple wave propagation formula, similar to do in the previous work⁹. Interested readers are referred to the Supplementary Methods for details. Wave overtopping is estimated using the wave parameters, storm surge levels and the breakwater database. Given that detailed designs of breakwaters are not available on a global scale, we first create a synthetic breakwater design per port based on engineering design principles (in particular, the crest height) and use these design criteria to estimate daily overtopping time series per port. Interested readers are referred to Supplementary Methods for the details of the methodology and Supplementary Fig. 6 for the result of the crest height of the breakwaters.

Physical asset damages and recovery time. Physical asset damages are evaluated for five natural hazards: earthquakes, TC wind, fluvial flooding, pluvial flooding and coastal flooding. We have developed separate methodologies for each hazard type, as explained below. To estimate physical asset damages, we follow the standard approach in risk modelling by overlaying the hazard layer with the geolocation of the asset and assign a damage value to that asset based on asset-specific and hazard-specific fragility curves and the maximum (re)construction costs of the asset⁴⁴. Moreover, we estimate the recovery time associated with repairing or reconstructing the asset, which results in downtime of the port. To estimate the overall port downtime, we consider only the essential port infrastructure and the critical infrastructure, as they are directly contributing to the operational functionality of the port (see ‘Port downtime’). Recovery curves relate the fraction of damage to the number of days of recovery. We adopt a simple area or length-weighted approach to estimate the port-wide fraction of damage. For instance, if 50% of the roads are 20% damaged, 20% of the roads are 100% damaged, and the other 30% remain intact, the road damage to the port is 30% ($0.5 \times 0.2 + 0.2 \times 1.0 + 0.3 \times 0.0$). An overview of the maximum damage values adopted is shown in Supplementary Table 1.

We use the earthquake hazard maps included in the UNISDR Global Assessment Report 2015⁴⁵, which are based on a fully probabilistic seismic hazard model. The hazard maps depict the severity of ground shaking measured in peak ground acceleration (PGA) in cm/s^2 and are available for five return periods (250, 475, 975, 1500 and 2475 years). Different fragility curves are defined for the different land-use types, which either reflect direct damage to the structure/buildings (e.g. warehouse, bulk and liquid) or to the quay walls (Container, General Cargo, RoRo). Moreover, earthquake fragility curves for the critical infrastructure assets are adopted (see Supplementary Table 1 for an overview of the sources). The earthquake recovery curves and maximum recovery days are based on FEMA’s 2020 HAZUS Earthquake Technical Manual⁴⁶. The maximum port recovery duration adopted corresponds well with the recovery of the port of Kobe after the 1995 earthquake, which took almost 2 years to fully recover⁴⁷.

The impact of TCs is measured only in terms of extreme wind speeds that affect port operations and cause damage to assets. To estimate the TC hazard, we make use of 10,000 years of synthetic TC paths per cyclone basin⁴⁸. Each path represents a plausible TC with location, wind speed, radius and pressure estimated every 6 h from its origin until full dissipation. To estimate the wind speed at the port, we use a parametric wind speed model based on the Holland wind speed profile⁴⁹, which is the most widely used parametric formula. We use the formulation of Lin and Chavas⁵⁰ to estimate the Holland parameter, with environmental pressure values taken from the AIR hurricane model⁵¹. Out of the port infrastructure, only industrial facilities, liquid terminals, bulk terminals, and warehouses are assumed to be prone to wind impacts. For the critical infrastructure, road and rail infrastructure is assumed to be unaffected, in line with⁵², while electricity and power plants are vulnerable to damage. Moreover, we include a fragility curve for ship-to-shore cranes, which are known to be susceptible to extreme winds. See Supplementary Table 1 for an overview of the fragility curves. Instead of using recovery curves for TC wind, we derive an empirical port recovery relationship. To estimate the duration a port is out of service due to a TC event, we fit a regression model based on observed port downtime due to TCs as reported in a port disruption database²⁴. This database includes 107 observations of port disruptions due to TCs leading to downtime across the world. The regression model we adopt includes the maximum wind speed, the duration (hours) above 15 and 35 m/s, the distance between the eye of the TC and the port, and three dummy variables to include whether a port has good/bad shelter, is large/small and has pilot assistance or not. The 15 and 35 m/s thresholds are adopted as they roughly correspond to the serviceability and ultimate limit thresholds of ship-to-shore cranes. We estimate the variables based on the historical TC paths derived from the ‘International Best

Track Archive for Climate Stewardship’ (IBTrACS) database (to match the TC to the one reported) and the method described above. The model fit is good ($R^2 = 0.75$), all variables are significant at $p = 0.1$ or lower except for the 15 m/s thresholds. The predicted and observed estimates are shown in Supplementary Fig. 7, including the uncertainty of the fitted parameters. We adopt this regression model to estimate the downtime for all synthetic TC events and derive empirical return periods. We use the uncertainty associated with the prediction for the sensitivity analysis (see ‘Sensitivity analysis’).

Global fluvial and pluvial flood hazard maps are obtained from JBA Consulting (<https://www.jbaconsulting.com>), which has created inundation maps for the port areas. Hazard maps for six return periods (20, 50, 100, 200, 500 and 1500 years) at 1-arcsecond resolution (~30 m) are used for this analysis. We would like to refer to Aerts et al.⁵³ for an overview of the JBA global river flood model and a comparison to other global river flood models. For fluvial flooding, we add protection standards from the FLOPROS database⁵⁴ to the data and truncate return periods below the protection standards as they will not result in flooding. No protection standards are added to the pluvial flooding risk calculations, as drainage infrastructure is often only protected against ~10-year pluvial flood events¹⁵, although some ports have higher engineering standards. However, given a lack of globally consistent data (and given that 20 years is the lowest return period), we do not adopt additional protection standards in the analysis. Fragility curves are based on a number of sources, as shown in Supplementary Table 1. The recovery curves adopted are similar as the earthquake recovery curves. However, the maximum recovery values are adjusted to reflect the known recovery durations of ports. A maximum port recovery of 120 days is used, which is based on the time needed to reconstruct the port of New Orleans⁵⁵ and the port of Mobile¹⁴ after Hurricane Katrina, whereas the road and rail maximum recovery durations are based on the time spent to recover flooded railway lines in Australia that affected port operations at Port Walcott and the Port of Hay Point for ~45 days²⁴.

Coastal flood hazard maps are used in most previous global coastal flood risk analysis^{12,23}. However, these coastal flood maps are not well suited for coastal flood risk analysis of ports. First, the digital elevation model (DEM) included in such analysis often has a low resolution and does not adequately capture the elevation of port terminals at the sea-land boundary. Previous research, for instance, illustrated the sensitivity of inundation of port facilities in the U.S. Virgin Islands due to errors in the DEM⁵⁶. Second, the EWL time series that is used for coastal inundation modelling includes assumptions on the EWL contributions (e.g. wave set-up) that are important for some ports but not for others (due to the presence of breakwaters). We, therefore, create our own EWL time series for ports based on the time series of different EWL components

$$EWL = Tide + Surge + SLA + WS$$

with Tide representing the daily tide, Surge the storm surge, SLA the sea-level anomalies and WS the wave set-up for the port. The tide and surge time series are based on daily values from the Global Tide and Surge Model for 1979–2018⁵⁷. The SLA are taken from satellite altimetry data (1993–2015) on a monthly time scale⁵⁸. The importance of WS depends on whether a port is exposed to breaking waves, and whether or not a breakwater is in place. In line with the wave overtopping, we assume that ports that are not exposed to overtopping are also not exposed to WS from breaking waves. We also assume that ports located more than 20 km from the coast are not exposed, since we cannot predict storm surges in tidal river channels or inland lakes. For port terminals that are exposed, the contribution of WS depends on the presence of a breakwater. If no breakwater is present, or a seawall is in place, we assumed WS to be 20% of the significant wave height ($0.2 \times H_s$) in line with the previous work⁵⁹. If a breakwater is present, the wave height inside the harbour area, the transmitted wave height, is equal to the outside wave height times the transmission coefficient K_t ($H_{s,t} = H_s \times K_t$). We estimated $H_{s,t}$ using the Goda formula⁶⁰, which is often used in practice

$$H_{s,t} = H_s * \frac{1}{2} \left[1 - \sin\left(\frac{\pi(R_c/H_s + \beta)}{2\alpha}\right) \right]$$

with R_c denoting the breakwater freeboard and K_t bounded between 0 and 1 with α and β equal to 2.0 and 0.5⁶⁰. R_c comes from the breakwater design established previously (Supplementary Fig. 6). To estimate the return periods of EWL (2, 5, 10, 20, 50, 100, 200, 500, 1000 and 5000), we used the GEV-6 largest method (fit a GEV function to the 6 largest values every year), as it was shown that this method does not overestimate nor underestimate EWL compared to other approaches⁶¹. In case this gives an unbounded fit, we used a GEV fitted to annual maximum EWL (GEV-A), or a Gumbel fitted to annual maxima if GEV-A gives unbounded results as well. To illustrate, the modelled 100-year EWL is shown in Supplementary Fig. 8. To estimate the flood extent per return period, we overlaid the modelled EWL with the elevation of the port and hinterland infrastructure. We used the JAXA AW3D30 DEM model⁶² with a 30 m horizontal resolution to perform the analysis. The JAXA AW3D30 DEM was found to be the best performing DEM compared to other global DEMs based on an analysis of multiple geographical regions⁶³, and is particularly good in capturing the sea-land boundary accurately⁶⁴. We adopt the same fragility curves and recovery estimates as used in pluvial and fluvial flood analysis. Coastal flood protection standards from Tiggeloven et al.⁶⁵ are used in the analysis in a similar fashion as in fluvial flood risk analysis.

Port downtime. To derive the port downtime associated with asset reconstruction, we perform a simple FTA based on the recovery duration of the port and critical infrastructure assets. An FTA captures how disruptions to the different components of the ports lead to a loss in functionality to the port as a whole. FTA has been used previously for detailed risk analysis of single ports¹⁴. Here, we adopted an FTA with the port terminals, cranes, road infrastructure, rail infrastructure, and electricity infrastructure as individual nodes in the failure tree. A representation of the fault tree is shown in Supplementary Fig. 10. A failure of any of the nodes (infrastructure components) can reduce the functionality of the port (called an ‘OR’ gate in FTA). In other words, if any of the subcomponents need to be restored, the port as a whole becomes operable as well, which is a simplified representation of reality but is essential to capture the local infrastructure interdependencies. If multiple components are facing restoration time, the ports face downtime until the component with the largest restoration time is restored, which is considered an upper bound of the expected restoration time. We perform this FTA analysis per hazard and event severity.

Logistics losses. The logistics losses as a result of downtime consist of three components: the loss to port and terminal operators, the loss to shippers and the loss to carriers. Here, we used a simplified approach to estimate the logistics losses due to downtime in line with previous work^{17,18}. First, the port authority or terminal operator has a direct economic loss when it cannot provide cargo loading/unloading services, for which they charge a fee per tonnes loaded or unloaded. The L_{port} can be written as

$$L_{port} = c_{(un)load} f \Delta T$$

With $c_{(un)load}$ denoting the port charge per tonnes loaded/unloaded (USD/tonnes), f the daily freight flow in tonnes, and ΔT the number of days of downtime. Second, the shipper incurs losses because goods need to be stored (inventory loss) and there is a monetary value associated with time (value of time). The inventory loss is equal to the inventory costs per tonnes, whereas the value of time is associated with the opportunity cost of the goods. In short, we can write $L_{shipper}$ as

$$L_{shipper} = I f \Delta T + VOT f \Delta T^2$$

With I denoting the inventory costs per tonnes (USD/tonnes) and VOT the value of time (USD/tonnes/day). Third, the carriers suffer economic losses due to the risk of late delivery ($L_{carrier}$). This is assumed to scale with the freight rate of the goods. In short

$$L_{carrier} = F f \Delta T$$

With F denoting the freight rate of cargo per tonnes (USD/tonnes). The total logistics losses are the summation of the three individual factors. The values of the loading/unloading rate, the inventory cost and the freight rate are based on previous work^{17,18}. In reality, however, these values can vary between ports and regions. We will therefore test the sensitivity of these values. The estimated value of time and daily freight flows (in tonnes) are obtained from the previous work¹.

Port-specific risk and trade risk. The port-specific risk includes (1) physical asset damages to port infrastructure, (2) physical asset damages to critical infrastructure and (3) additional logistics losses due to downtime. For (1) and (2), we first aggregated the damages to the port-level per return period and hazard. Per hazard, we calculated the risk, expressed in terms of annual expected damages (\$US/year), by applying the trapezoidal rule. We sum the risk values across the hazard types, thereby ignoring any form of dependency or non-linearity between hazards. We then add the logistics losses associated with the operational downtime to the port-specific risk estimates.

Trade risk is defined as the amount of maritime trade (in monetary value) that is at risk of being disrupted annually. We can use the derived downtime estimates per natural hazard and severity to find the annual expected downtime (number of days per year) by applying the trapezoidal rule, and aggregating the downtime across hazards. The downtime associated with the operational thresholds is also added to this. We used this downtime metric to estimate the trade risk by multiplying the annual expected downtime with the estimated average daily trade value in a port, which is based on the previous work¹.

Sensitivity analysis. A number of assumptions and generalisations are made in the various model components. In order to capture the uncertainty in input parameters, and evaluate the sensitivity of the results to these uncertainties, we performed a large-scale sensitivity analysis. To do this, we adopted a variance-based sensitivity analysis (Sobol sensitivity analysis)⁶⁶, which is implemented in the SALib python package⁶⁷. For every input parameter specified in Supplementary Table 1, we added an uncertainty range to the parameter (see Supplementary Table 1) and sampled 10,000 parameters from a uniform distribution function, except for the TC regression uncertainty, for which we use a normal distribution. We performed the sensitivity analysis for both the global estimates (port-specific risk and trade risk), as well as on a port level (by running the algorithm for every port individually). This allowed us to explore the main drivers for the variance of the results.

To evaluate the sensitivity of the resilience parameters, we sum the resulting contributions of a number of resilience-related input parameters. For the

'Operational' indicator, we summed all input parameters related to the operational risk (e.g. thresholds and breakwater design parameter). For the 'Engineering standards', we summed the sensitivity measures of the depth-damage curves. The 'Recovery' indicator reflects all input parameters that affect the recovery duration, i.e. the recovery curves and the maximum recovery duration.

Data availability

The port asset database created and the output of the risk analysis to reproduce the results are available from Mendeley Data (<https://doi.org/10.17632/kdyt24tsh5.1>). All input data, except the pluvial and fluvial hazard maps (which are licensed from JBA Consulting), are publicly available at the various sources mentioned in the article.

Code availability

The code to run the analysis is available on [GitHub](#).

Received: 24 February 2022; Accepted: 6 December 2022;

Published online: 12 January 2023

References

- Verschuur, J., Koks, E. E. & Hall, J. W. Ports' criticality in international trade and global supply-chains. *Nat. Commun.* **13**, 4351 (2022).
- Rose, A. & Wei, D. Estimating the economic consequences of a port shutdown: the special role of resilience. *Econ. Syst. Res.* **25**, 212–232 (2013).
- Becker, A. H. et al. A note on climate change adaptation for seaports: a challenge for global ports, a challenge for global society. *Clim. Change* **120**, 683–695 (2013).
- FEMA. *Hurricane Ike Impact Report*. (2008).
- Chatterton, J. et al. *The costs and impacts of the winter 2013 to 2014 floods*. (2016).
- Verschuur, J., Pant, R., Koks, E. & Hall, J. A systemic risk framework to improve the resilience of port and supply-chain networks to natural hazards. *Marit. Econ. Logist.* <https://doi.org/10.1057/s41278-021-00204-8> (2022).
- Levermann, A. Climate economics: make supply chains climate-smart. *Nature* **506**, 27–29 (2014).
- World Bank. Private Participation in Infrastructure Database. *Port Sector Snapshot* (2021). <https://ppi.worldbank.org/en/snapshots/sector/ports>. Accessed June 4, 2021.
- Izaguirre, C., Losada, I. J., Camus, P., Vigh, J. L. & Stenek, V. Climate change risk to global port operations. *Nat. Clim. Chang.* **11**, 14–20 (2021).
- Allen, T. R., McLeod, G. & Hutt, S. Sea level rise exposure assessment of U.S. East Coast cargo container terminals. *Marit. Policy Manag.* **00**, 1–23 (2021).
- ITF. *ITF Transport Outlook 2019*. (OECD, 2019). https://doi.org/10.1787/transport_outlook-en-2019-en
- Christodoulou, A., Christidis, P. & Demirel, H. Sea-level rise in ports: a wider focus on impacts. *Marit. Econ. Logist.* **21**, 482–496 (2019).
- Aerts, J. C. J. H. et al. Pathways to resilience: adapting to sea level rise in Los Angeles. *Ann. N. Y. Acad. Sci.* **1427**, 1–90 (2018).
- Abdelhafez, M. A., Ellingwood, B. & Mahmoud, H. Vulnerability of seaports to hurricanes and sea level rise in a changing climate: a case study for mobile, AL. *Coast. Eng.* **167**, 103884 (2021).
- Canevari, L. et al. *Port of Manzanillo: Climate Risk Management*. (2015).
- Stenek, V. et al. Climate Risk and Business: Ports: Terminal Marítimo Muelles el Bosque, Cartagena Colomb. 179 (2011).
- Zhang, Y. et al. Economic impact of typhoon-induced wind disasters on port operations: a case study of ports in China. *Int. J. Disaster Risk Reduct.* **50**, 101719 (2020).
- Zhang, Y. & Lam, J. S. L. Estimating the economic losses of port disruption due to extreme wind events. *Ocean Coast. Manag.* **116**, 300–310 (2015).
- LaRocco, L. A. Suez Canal blockage is delaying an estimated \$400 million an hour in goods. *Transportation* (2021).
- Linkov, I. et al. Changing the resilience paradigm. *Nat. Clim. Chang.* **4**, 407–409 (2014).
- Rose, A., Wei, D. & Paul, D. Economic consequences of and resilience to a disruption of petroleum trade: the role of seaports in U.S. energy security. *Energy Policy* **115**, 584–615 (2018).
- Koks, E. E. & Thissen, M. A multiregional impact assessment model for disaster analysis. *Econ. Syst. Res.* **28**, 429–449 (2016).
- Koks, E. E. et al. A global multi-hazard risk analysis of road and railway infrastructure assets. *Nat. Commun.* **10**, 2677 (2019).
- Verschuur, J., Koks, E. E. & Hall, J. W. Port disruptions due to natural disasters: insights into port and logistics resilience. *Transp. Res. Part D Transp. Environ.* **85**, 102393 (2020).
- De Moel, H., Asselman, N. E. M. & Aerts, J. C. J. H. Uncertainty and sensitivity analysis of coastal flood damage estimates in the west of the Netherlands. *Nat. Hazards Earth Syst. Sci.* **12**, 1045–1058 (2012).
- Asariotis, R., Benamara, H. & Mohos-Naray, V. Port industry survey on climate change impacts and adaptation. *United Nations Conference on Trade and Development* **66** (2017).
- Bevaqua, E. et al. Higher probability of compound flooding from precipitation and storm surge in Europe under anthropogenic climate change. *Sci. Adv.* **5**, 1–8 (2019).
- de Ruiter, M. C. et al. Why we can no longer ignore consecutive disasters. *Earth's Futur.* **8**, 1–19 (2020).
- Davies, G. et al. A global probabilistic tsunami hazard assessment from earthquake sources. *Geol. Soc. Lond. Spec. Publ.* **456**, 219–244 (2018).
- Otake, T., Chua, C. T., Suppasri, A. & Imamura, F. Justification of possible casualty-reduction countermeasures based on global tsunami hazard assessment for tsunami-prone regions over the past 400 years. *J. Disaster Res.* **15**, 490–502 (2020).
- Muhari, A., Charvet, I., Tsuyoshi, F., Suppasri, A. & Imamura, F. Assessment of tsunami hazards in ports and their impact on marine vessels derived from tsunami models and the observed damage data. *Nat. Hazards* **78**, 1309–1328 (2015).
- Hanson, S. E. & Nicholls, R. J. Demand for Ports to 2050: climate policy, growing trade and the impacts of sea-level rise. *Earth's Futur.* **8**, 1–13 (2020).
- Singh, S. J. et al. Socio-metabolic risk and tipping points on islands. *Environ. Res. Lett.* **17**, 065009 (2022).
- Asian Development Bank. *Trade and Maritime Transport Trends in the Pacific*. (2020).
- Meijer, J. R., Huijbregts, M. A. J., Schotten, K. C. G. J. & Schipper, A. M. Global patterns of current and future road infrastructure. *Environ. Res. Lett.* **13** (2018).
- Arderne, C., Zorn, C., Nicolas, C. & Koks, E. E. Predictive mapping of the global power system using open data. *Sci. Data* **7**, 1–12 (2020).
- Byers, L. et al. *A Global Database of Power Plants*. World Resources Institute (2019).
- Oberschelp, C., Pfister, S., Raptis, C. E. & Hellweg, S. Global emission hotspots of coal power generation. *Nat. Sustain.* **2**, 113–121 (2019).
- Verschuur, J., Koks, E. E. & Hall, J. W. Global economic impacts of COVID-19 lockdown measures stand out in high-frequency shipping data. *PLoS ONE* **16**, e0248818 (2021).
- Monioudi, I. et al. Climate change impacts on critical international transportation assets of Caribbean Small Island Developing States (SIDS): the case of Jamaica and Saint Lucia. *Reg. Environ. Chang.* **18**, 2211–2225 (2018).
- Hersbach, H. et al. The ERA5 Global Reanalysis. *Q. J. R. Meteorol. Soc.* <https://doi.org/10.1002/qj.3803> (2020).
- Sierra, J. P., Casanovas, L., Mössö, C., Mestres, M. & Sánchez-Arcilla, A. Vulnerability of Catalan (NW Mediterranean) ports to wave overtopping due to different scenarios of sea level rise. *Reg. Environ. Chang.* **16**, 1457–1468 (2016).
- EurOtop. *Manual on Wave Overtopping of Sea Defences and Related Structures. an Overtopping Manual Largely Based on European Research, But for Worldwide Application*. (2018).
- Meyer, V. et al. Review article: assessing the costs of natural hazards-state of the art and knowledge gaps. *Nat. Hazards Earth Syst. Sci.* **13**, 1351–1373 (2013).
- UNISDR. *Annex 1: GAR Global Risk Assessment: Data, Methodology, Sources and Usage*. 1–37 (2015).
- FEMA. *Hazus Earthquake Model Technical Manual. HAZUS 4.2 SP3* (2020).
- Chang, S. E. Disasters and transport systems: loss, recovery and competition at the Port of Kobe after the 1995 earthquake. *J. Transp. Geogr.* **8**, 53–65 (2000).
- Bloemendaal, N. et al. Generation of a global synthetic tropical cyclone hazard dataset using STORM. *Sci. Data* **7**, 40 (2020).
- Holland, G. J. An analytic model of the wind and pressure profiles in hurricanes. *Mon. Weather Rev.* **108**, 1212–1218 (1980).
- Lin, N. & Chavas, D. On hurricane parametric wind and applications in storm surge modeling. *J. Geophys. Res. Atmos.* **117**, 1–19 (2012).
- Butke, J. *The Pressure's On: Increased Realism in Tropical Cyclone Wind Speeds through Attention to Environmental Pressure*. (2012).
- Miyamoto International. *Overview of Engineering Options for Increasing Infrastructure Resilience*. (2019).
- Aerts, J., Uhlemann-Elmer, S., Eilander, D. & Ward, P. Global flood hazard map and exposed GDP comparison: a China case study. *Nat. Hazards Earth Syst. Sci. Discuss.* 1–26 <https://doi.org/10.5194/nhess-2020-1> (2020).
- Scussolini, P. et al. FLOPROS: an evolving global database of flood protection standards. *Nat. Hazards Earth Syst. Sci.* **16**, 1049–1061 (2016).

55. Rousset, L. & Ducruet, C. Disruptions in spatial networks: a comparative study of major shocks affecting ports and shipping patterns. *Netw. Spat. Econ.* **20**, 423–447 (2020).
56. Bove, G., Becker, A., Sweeney, B., Vousdoukas, M. & Kulp, S. A method for regional estimation of climate change exposure of coastal infrastructure: case of USVI and the influence of digital elevation models on assessments. *Sci. Total Environ.* **710**, 136162 (2020).
57. Muis, S. et al. A high-resolution global dataset of extreme sea levels, tides, and storm surges, including future projections. *Front. Mar. Sci.* **7**, 1–15 (2020).
58. Ablain, M. et al. Improved sea level record over the satellite altimetry era (1993–2010) from the Climate Change Initiative project. *Ocean Sci.* **11**, 67–82 (2015).
59. Vousdoukas, M. I. et al. Global probabilistic projections of extreme sea levels show intensification of coastal flood hazard. *Nat. Commun.* **9**, 2360 (2018).
60. Goda, Y., Takeda, H. & Moriya, Y. *Laboratory Investigation on Wave Transmission over Breakwaters*. (1967).
61. Wahl, T. et al. Understanding extreme sea levels for broad-scale coastal impact and adaptation analysis. *Nat. Commun.* **8**, 1–12 (2017).
62. Takaku, J., Tadono, T., Doutsu, M., Ohgushi, F. & Kai, H. Updates of aw3d30' alos global digital surface model with other open access datasets. *Int. Arch. Photogramm. Remote Sens. Spat. Inf. Sci.* **43**, 183–190 (2020).
63. Uuemaa, E., Ahi, S., Montibeller, B., Muru, M. & Kmoch, A. Vertical accuracy of freely available global digital elevation models (Aster, aw3d30, merit, tandem-x, srtm, and nasadem). *Remote Sens.* **12**, 1–23 (2020).
64. Almar, R. et al. A global analysis of extreme coastal water levels with implications for potential coastal overtopping. *Nat. Commun.* **12**, 3775 (2021).
65. Tiggeeloven, T. et al. Global-scale benefit-cost analysis of coastal flood adaptation to different flood risk drivers using structural measures. *Nat. Hazards Earth Syst. Sci.* **20**, 1025–1044 (2020).
66. Saltelli, A. Making best use of model evaluations to compute sensitivity indices. *Comput. Phys. Commun.* **145**, 280–297 (2002).
67. Herman, J. & Usher, W. SALib: an open-source Python library for Sensitivity Analysis. *J. Open Source Softw.* **2**, 97 (2017).

Acknowledgements

The authors would like to thank JBA consulting for the provision of the global fluvial and pluvial hazard maps and Sanne Muis for providing the output of the Global Tide and Surge Reanalysis model. We would also like to thank those who provided data and comments to this work, in particular the International Finance Corporation (IFC) and five port experts (from port authorities and specialised consultancies). J.V. acknowledges funding from the Engineering and Physical Sciences Research Council (EPSRC) under grant number EP/R513295/1. E.E.K. is supported by the Netherlands Organisation for Scientific Research NOW (Grant no. VI.Veni.194.033).

Author contributions

J.V. conceptualised the research, performed the analysis, and led the writing of the manuscript. E.E.K. conceptualised the research, provided input and helped write the paper. S.L. processed the climate reanalysis data and helped write the paper. J.W.H. conceptualised the research, provided input and helped write the paper. All authors provided input to the draft and contributed to the writing of the final paper.

Competing interests

The authors declare no competing interests.

Additional information

Supplementary information The online version contains supplementary material available at <https://doi.org/10.1038/s43247-022-00656-7>.

Correspondence and requests for materials should be addressed to Jasper Verschuur.

Peer review information *Communications Earth & Environment* thanks Jiayi Fang, Constance Chua and the other, anonymous, reviewer(s) for their contribution to the peer review of this work. Primary Handling Editors: Adam Switzer, Joe Aslin. Peer reviewer reports are available.

Reprints and permission information is available at <http://www.nature.com/reprints>

Publisher's note Springer Nature remains neutral with regard to jurisdictional claims in published maps and institutional affiliations.



Open Access This article is licensed under a Creative Commons Attribution 4.0 International License, which permits use, sharing, adaptation, distribution and reproduction in any medium or format, as long as you give appropriate credit to the original author(s) and the source, provide a link to the Creative Commons license, and indicate if changes were made. The images or other third party material in this article are included in the article's Creative Commons license, unless indicated otherwise in a credit line to the material. If material is not included in the article's Creative Commons license and your intended use is not permitted by statutory regulation or exceeds the permitted use, you will need to obtain permission directly from the copyright holder. To view a copy of this license, visit <http://creativecommons.org/licenses/by/4.0/>.

© The Author(s) 2023